Biocybernetics and Biomedical Engineering 44 (2024) 9–19

Contents lists available at ScienceDirect

Biocybernetics and Biomedical Engineering

journal homepage: www.elsevier.com/locate/bbe

Hollow fiber bioreactor with genetically modified hepatic cells as a model of biologically active function block of the bioartificial liver

Malgorzata Jakubowska [a], Monika Joanna Wisniewska [a], Agnieszka Wencel [a], Cezary Wojciechowski [b], Monika Gora [c], Krzysztof Dudek [d], Andrzej Chwojnowski [b], Beata Burzynska [c], Dorota Genowefa Pijanowska [a], Krzysztof Dariusz Pluta [a,*]

[a] Department of Hybrid and Analytical Microbiosystems, Nalecz Institute of Biocybernetics and Biomedical Engineering, Polish Academy of Sciences, Warsaw, Poland
[b] Department of Biomaterials and Biotechnological Systems, Nalecz Institute of Biocybernetics and Biomedical Engineering, Polish Academy of Sciences, Warsaw, Poland
[c] Institute of Biochemistry and Biophysics, Polish Academy of Sciences, Warsaw, Poland
[d] Department of General, Transplant & Liver Surgery, University Medical Center, Medical University of Warsaw, Poland

ARTICLE INFO

Keywords:
Liver failure
Hepatic cell culture
Human hepatocellular carcinoma (HCC)
Genetically modified cells
Hollow fiber bioreactor
Bioartificial liver (BAL)

ABSTRACT

Chronic liver disease and cirrhosis, that can lead to liver failure, are major public health issues, with liver transplantation as the only effective treatment. However, the limited availability of transplantable organs has spurred research into alternative therapies, including bioartificial livers. To date, liver hybrid support devices, using porcine hepatocytes or hepatoma-derived cell lines, have failed to demonstrate efficacy in clinical trials.

Here, for the first time, we report the construction of a model of biologically active function block of bioartificial liver based on a hollow fiber bioreactor populated with genetically modified hepatic cells. For comprehensive comparison the culturing of hepatic cells was carried out in both static and dynamic conditions in a medium that flowed through porous polysulfone capillaries. The most crucial parameters, such as cell viability, glucose consumption, albumin secretion and urea production, were analyzed in static conditions while glucose usage and albumin production were compared in dynamic cell cultures. This model has the potential to improve the development of bioartificial liver devices and contribute to the treatment of patients with impaired liver function.

1. Introduction

The liver is the body metabolic factory that performs over 500 functions important for maintaining the homeostasis of an organism. Despite its ability to regenerate and unique capacity to regrow, liver damage and diseases may lead to chronic or acute liver failure (ALF). As the mortality rate of chronic liver diseases reaches 2 million deaths annually, they constitute a serious global public health problem [1]. On the other hand, ALF, a rather less common condition, with a lethality of over 80 % makes treatment of patients much more difficult [2]. To date, the only effective treatment for fulminant hepatic failure is liver transplantation (LT). However, the LT technique is not flawless and brings up a substantial set of challenges. The major limitation for LT remains an organ shortage, which accounts for a large proportion of wait list mortality. Therefore, scientists and clinicians have developed several experimental therapies that are alternatives to organ transplantation and are designated as solutions bridging the time until transplantation or supporting organ regeneration. The most encouraging of these therapeutic techniques are associated with the use of hepatocytes or hepatocyte-like cells. Research into cell-based liver therapy is developing by two paths: hepatocyte transplantation (HT) and the construction of bioartificial liver (BAL) devices [3,4]. These techniques, along with the use of extracorporeal liver support devices, could represent feasible alternatives to LT [5].

Liver support devices, also known as artificial livers, have been clinically tested over the past three decades. Nonbiological liver assist techniques rely on blood detoxification using sorbents (charcoal or resins), hemodialysis, hemofiltration, and more recently, plasma exchange or albumin dialysis [6]. These devices are effective in clearing water-soluble, small and middle molecular weight toxins from the blood. However, sorbents are not very much capable of removing proteins, including inhibitors of hepatic regeneration and mediators of

* Corresponding author at: Nalecz Institute of Biocybernetics and Biomedical Engineering PAS, Ks. Trojdena 4 st. 02-109, Warsaw, Poland.
E-mail address: kpluta@ibib.waw.pl (K. Dariusz Pluta).

https://doi.org/10.1016/j.bbe.2023.11.003
Received 4 August 2023; Received in revised form 15 November 2023; Accepted 28 November 2023
Available online 7 December 2023

inflammation. Moreover, nonbiological liver assist devices cannot substitute biosynthetic and metabolic liver functions and thus failed to meet expectations in randomized controlled clinical trials, as they had no impact on the survival rate in the unselected population of patients with ALF [7,8].

In the case of cell-based therapeutic strategies, an adequate source of liver parenchymal cells is a key issue [9]. The best cells to be used in such applications are isolated human hepatocytes. New protocols for human hepatocyte isolation are being developed, and the capabilities of these cells are still being examined [10,11]. Unfortunately, as in the case of organ transplantation, the main problem is the limited availability of good-quality human liver tissue. Other limitations for the use of human isolated hepatocytes for liver therapies are as follows: cells do not divide and rapidly dedifferentiate *ex vivo*, which leads to the loss of their specific functions, and donor-to-donor variability may affect therapeutic outcomes [12]. Thus, alternative liver cell sources have gained much interest in recent years. In addition to the use of well-studied porcine hepatocytes and human hepatocellular carcinoma (HCC)-derived cell lines - HepaRG, HepG2, and its subclone C3A, they are as follows: hepatocyte-like cells obtained from stem cells, hepatic progenitor cells, and induced hepatocyte–like (iHep) cells differentiated from induced pluripotent stem cells (iPSCs). Even though these alternative sources of hepatic cells can bring hope, the functionality and efficacy of primary human hepatocytes are still irreplaceable.

The two most advanced bioartificial livers, HepatAssist (HepaMate™; HepaLife, USA) and ELAD (*Extracorporeal Liver Assist Device*; Vital Therapies Inc., USA), utilize polysulfone hollow fiber bioreactors populated with hepatic cells placed in the extracapillary space of the cartridges. These culture modules serve as biologically active function block of the BAL (BAFBBAL). The former hybrid device is based on porcine primary hepatocytes, and the latter is based on C3A cells [13,14]. The use of porcine hepatocytes may face problems such as unexpected immune response, protein–protein incompatibility or potential zoonotic disease transmission. Considering the above, the cells of choice for current BAL applications are human liver tumor-derived cell lines characterized by a very high proliferation rate and phenotypic stability. However, this source of hepatic cells is also not free of defects. Despite the fact that HepG2/C3A HCC cells possess a number of features of human hepatocytes, they have some metabolic deficiencies. First, HCC cells are characterized by decreased activity of cytochrome P450 isoenzymes. Second, they do not metabolize ammonia efficiently because their urea cycle is impaired. It has been suggested that because of a complete lack or low levels of the expression of arginase I (*ARG*1) and ornithine transcarbamylase (*OTC*) genes, the activity of the proteins involved in these enzymatic reactions is downregulated [15–18]. As has been recently demonstrated, HCC cells consistently repress urea cycle gene expression and thus become auxotrophic for exogenous arginine [19]. The limited metabolic capacity of the cells used in ELAD could be a reason for its failure in randomized controlled clinical trials [20].

Here, we present our research results on different cell types that could be used in BAFBBAL. First, we constructed the BAFBBAL model based on a hollow fiber bioreactor utilizing semipermeable polysulfone membranes. Such a cell culture module was then used for culturing C3A cells and their derivatives, genetically modified with lentiviral vectors carrying transgenes coding for human arginase I and ornithine transcarbamylase, C3A_AO [21] and its newer version C3A_AO_P2A. For comparison, the cultures were carried out in monolayers and, to reproduce conditions present in hollow fiber BAL bioreactors, in dynamic conditions. Therefore, we postulate such a dynamic culture of genetically modified HCC cells as a novel method of BAL construction. This is because these cells cultivated with medium flowing through capillaries secrete more albumin and perform better overall than corresponding cultures carried out in static conditions.

2. Materials and methods

2.1. Cells and cell culture

Human hepatocellular carcinoma - C3A (CRL-10741), human osteosarcoma - HOS (CRL-1543), and human embryonic kidney 293 T - HEK293T (CRL-11268) cell lines were obtained from the American Type Culture Collection (ATCC, Manassas, VA, USA). The cells were cultured under standard conditions (37 °C; atmosphere containing 5 % CO_2) in a high glucose DMEM (Dulbecco's Modified Eagle Medium, Sigma Aldrich, Poznan, Poland) supplemented with a 10 % fetal bovine serum - FBS (ATCC, Manassas, VA, USA) and 1 % nonessential amino acids solution (Biological Industries Inc., Beit-Haemek, Israel). The C3A_AO cell line, with integrated additional copies of the h*ARG1* and h*OTC* genes (transgenes), was obtained as described previously using two lentiviral vectors [21]. In turn, the newly generated C3A_AO_P2A cell line was obtained by the transduction of C3A cells with the single lentiviral vector carrying both transgenes combined in one transcriptional cassette. Details concerning the construction of the new generation of the genetically modified cell line are presented in the Supplementary materials. Human liver cell isolate was obtained as described elsewhere [10]. HOS cells were used as a negative control for physiological tests of hepatic cells.

2.2. Determination of gene expression using RT-qPCR

C3A, C3A_AO, and C3A_AO_P2A cells were seeded into 6-well plates at a density of $1{\cdot}10^6$ per well in standard medium and cultured for one day. The next day, the cells were treated with 40 mM NH_4Cl for 24 h. Then, the RNA was isolated with a Total RNA kit (A&A Biotechnology, Gdynia, Poland). Reverse transcription was conducted from 400 ng of total RNA using a QuantiTect Reverse Transcription Kit (QIAGEN, Hilden, Germany). The RT-qPCR analysis was performed using a LightCycler®480 System and a LightCycler®480 FastStart SYBR Green I Master mix (Roche Diagnostics GmbH, Mannheim, Germany). Each sample was run in triplicate. *GAPDH* and *RPL13A* were used as reference genes. All steps concerning RT-qPCR experiments were performed in accordance with MIQE guidelines [22]. For data analysis, the Pfaffl model [23] and relative expression (REST 2009) were used. The RT-qPCR details concerning primers and reaction conditions are provided in Supplementary Table 3.

2.3. Determination of albumin secretion using immunoenzymatic method - ELISA test

The C3A, C3A_AO, C3A_AO_P2A, and HOS cell lines were seeded at a density of $5{\cdot}10^4$ cells per well of a 12-well plate and grown in standard culture medium for 12 days. Every third day, the medium samples were collected and stored at −20 °C. The concentration of human serum albumin secreted by the analyzed cell lines was measured using a sandwich enzyme-linked immunosorbent assay (ELISA) with a quantitation kit (Bethyl Laboratories, Inc., Montgomery, TX, USA) and a microplate reader Synergy HT (BioTek, Winooski, VT, USA). The amounts of albumin were expressed in nanograms per $1{\cdot}10^3$ counted cells (the list of antibodies used is presented in Supplementary Table 1).

2.4. Determination of urea production

The C3A, C3A_AO, and C3A_AO_P2A cell lines were seeded at a density of $2{\cdot}10^6$ cells per well in a 6-well plate and grown in standard culture medium. The next day, cells were treated with 40 mM NH_4Cl for 24 h. After this, the medium was replaced with DMEM supplemented with 1 % FBS and 1 % nonessential amino acids and incubated for another 24 h. Then, the medium samples were collected and stored at −20 °C. Subsequently, the cell lysates were prepared and stored at −20 °C. To determine urea production, measurement of concentrations

of this substance both in conditioned medium samples and in cell lysates was conducted using a QuantiChrom Urea Assay Kit (BioAssay, Hayward, CA, USA) in accordance with the manufacturer's recommendations. Briefly, a 200 μL mixture of reagents A and B (in a ratio of 1:1) was added to 50 μL of sample and incubated for 50 min at RT. Absorbance was measured at 430 nm using a Synergy HT spectrophotometer (BioTek, Winooski, VT, USA).

2.5. Determination of the cytotoxic effect of NH_4Cl

2.5.1. Albumin secretion (ELISA test)

The C3A, C3A_AO, C3A_AO_P2A, and HOS cell lines were seeded at a density of $3{\cdot}10^6$ cells per T25 flask and grown in standard culture medium. The next day, the cells were treated with 20 mM or 40 mM ammonium chloride. Untreated cells were used as a control. After 24 h, the culture medium was replaced with fresh medium. After three days, the medium samples were collected and stored at −20 °C. Determination of albumin concentration was performed as described above.

2.5.2. Cell viability

The C3A, C3A_AO, C3A_AO_P2A, and HOS cell lines were seeded at a density of $1.5{\cdot}10^5$ cells per well of a 12-well plate and grown in standard culture medium for 3 days. Then, the cells were treated with 20 mM or 40 mM NH_4Cl for 24 h. Untreated cells were used as a control. The next day, the cell viability after staining with propidium iodide (PI) at a final concentration of 5 μg/ml was determined using a FACSCanto II flow cytometer (Becton Dickinson, Warsaw, Poland).

2.5.3. Mitochondrial activity (MTT assay)

The C3A, C3A_AO, C3A_AO_P2A, and HOS cell lines were seeded at a density of $3{\cdot}10^4$ cells per well of a 96-well plate and grown in standard culture medium. The next day, cells were treated with 20 mM, 40 mM or 60 mM NH_4Cl for 24 h. Then, the culture media were replaced with fresh media and incubated for another 24 h. Thereafter, 2-(4,5-dimethylthiazol-2-yl)-2,5-diphenyltetrazolium bromide (MTT, Sigma Aldrich, Poznan, Poland) at a final concentration of 0.25 mg/mL was added and incubated at 37 °C for 2 h. Absorbance was read at 570 nm using a Synergy HT spectrophotometer (BioTek, Winooski, VT, USA).

2.6. Determination of glucose consumption

The glucose concentration in the culture medium was measured using a commercial kit (BioMaxima, Lublin, Poland) according to the manufacturer's recommendations. Briefly, 2 μL of analyzed sample or standard was added to 200 μL of the colored reagent and incubated for 10 min at RT. Absorbance was read at 505 nm using a Synergy HT spectrophotometer (BioTek, Winooski, VT, USA).

2.7. Determination of the structure of the polysulfone capillary membrane

The characterization of the polysulfone membrane was conducted using a scanning electron microscope TM-1000 (SEM; Hitachi-High Technologies, Tokyo, Japan). Before analysis, capillaries were coated with gold for 90 s using a Sputter Coater Emitech K550X (Quorum Technologies, Ashford, Great Britain). Then, the structure of the polysulfone membrane was analyzed, and the pore size, as well as the internal and external diameters, were determined.

2.8. Retention measurement

Retention for bovine albumin (Fluka, Charlotte, NC, USA) was measured spectrophotometrically. First, a solution of bovine albumin at a concentration of 1 g/L was prepared. The obtained solution was passed through the module, and the permeate and retentate were collected. The absorbance of bovine albumin in both collected fractions was measured using a Hitachi U-3010 (Hitachi-High Technologies, Tokyo, Japan) spectrophotometer at a wavelength of 278 nm. The concentration of bovine albumin was determined from the calibration curve. The retention of polystyrene microspheres was measured using flow cytometry. Red fluorescent microspheres with particle sizes of 100 nm, 200 nm, and 500 nm (EPRUI Biotech, Suzhou, China) and microspheres with mixed fluorescence (red and green) with particle sizes of 2 μm and 3 μm (Becton Dickinson, Warsaw, Poland) were passed through the module, and the permeate and retentate were collected. Then, the number of events in both fractions was measured using a FACSCanto II flow cytometer (Becton Dickinson, Warsaw, Poland).

2.9. Construction of system for dynamic culture (model of BAFBBAL)

The heart of the dynamic culture system (model of biologically active function block of the BAL, BAFBBAL) constitutes the hollow fiber bioreactor (culture module), which was self-constructed using 20 semipermeable polysulfone capillary membranes (Vestergaard Frandsen, Lozanna, Switzerland). Its culture surface area is ca. 22 cm^2. The capillary membranes have a pore size of 0.2 μm. To construct the BAFBBAL model, a peristaltic pump, tubing, oxygenator (bubble trap), medium reservoir, needles, adapters, and connectors were used (Fig. 1). Before construction, the hollow fiber bioreactor was pasteurized twice (2 h, 60 °C). The tubing for the peristaltic pump was sterilized in an autoclave. The rest of the tubing and oxygenator were purchased in a sterile package. The needles, adapters, and connectors were sterilized in an autoclave or using 70 % ethanol solution.

2.10. Optimization of process parameters associated with dynamic culture

The optimization of two parameters connected with dynamic culture was conducted using the C3A cell line. The impact of two different flow rates (5 mL/min and 10 mL/min) and two different seeding densities ($0.5{\cdot}10^6$ or $5{\cdot}10^6$ of cells per bioreactor) on glucose consumption and albumin synthesis was evaluated.

2.11. Culture of human HCC cells in dynamic conditions

The day before seeding, sterile PBS was passed through the system and circulated for 24 h in the incubator (37 °C; atmosphere containing 5 % CO_2). The next day, the bottle with PBS was replaced with standard culture medium. After that, $5{\cdot}10^6$ cells were seeded on the extracapillary space of the membranes. For cell attachment to the membrane surface, the hollow fiber bioreactor was rotated by 180 degrees every 5 min for 1

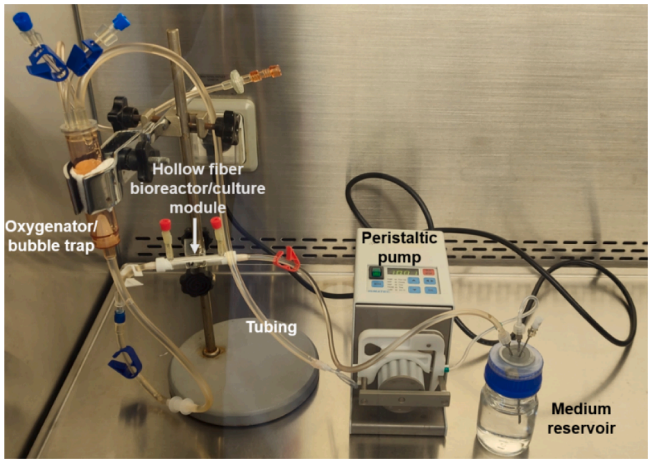

Fig. 1. Construction of BAFBBAL. Photograph of the constructed system for dynamic cell culture (model of the biologically active function block of bioartificial liver, BAFBBAL). A hollow fiber bioreactor was set as the heart of the developed system.

h. After that time, the peristaltic pump was turned on (flow rate: 10 mL/min). As a control for dynamic conditions, the same number of cells was seeded on a T25 flask (static culture carried on in 6 mL of medium). The cell culture lasted for 12 days. On days 2, 5, 7, 9, and 12, samples from dynamic and static conditions were collected and used for the determination of albumin secretion and glucose consumption. Cell viability at the end of the culture was determined using the trypan blue exclusion method.

2.12. Statistical data analysis

Data are expressed as the mean values and standard deviations (±SD). Statistical analysis was performed with Statistica 10 software (StatSoft Inc., Tulsa, OK, USA). Multivariate analysis of variance (MANOVA or ANOVA), followed by Duncan's *post hoc* test, was used to compare the means of 3 or more groups. A value of $p < 0.05$ or less was considered statistically significant (values of statistical significance for each experiment are provided in Supplementary Tables 4, 5, 6, and 7).

3. Results

3.1. Comparison of gene expression in HCC cells at the mRNA level

Determination of gene expression in C3A, C3A_AO, and C3A_AO_P2A cells was conducted using RT-qPCR analysis. The obtained results showed that the expression of the *ARG1* transgene was 34.5-fold ($p < 0.001$) higher in C3A_AO_P2A cells than in C3A_AO cells and 42.5-fold ($p = 0.022$) higher when comparing these cell lines after incubation with 40 mM NH_4Cl. A similar effect was observed for the *OTC* transgene. The expression of this gene was 43.9-fold ($p < 0.001$) higher in C3A_AO_P2A cells than in the older version of genetically modified cells and 49.4-fold ($p = 0.025$) higher when comparing these cell lines after incubation with 40 mM NH_4Cl. When the same cell lines were analyzed after ammonium chloride treatment and without treatment, for the C3A_AO_P2A cell line, the expression of *ARG1* and *OTC* transgenes was 2.1-fold ($p = 0.024$) and 1.9-fold ($p = 0.015$) higher, respectively. Similarly, for C3A_AO cells, the mRNA levels of *ARG1* and *OTC* were 1.7-fold ($p = 0.036$) and 1.7-fold ($p < 0.001$) higher, respectively (Fig. 2a). In turn, for unmodified C3A cells, the levels of *ARG1* and *OTC* transcripts were under the detection limit.

In the case of albumin, the expression of the gene was 2.7-fold and 1.9-fold higher when C3A_AO cells were compared with C3A_AO_P2A and C3A cell lines, respectively (p not shown when greater than 0.05). In turn, the mRNA levels of the analyzed gene in C3A_AO_P2A cells was decreased (0.7-fold) in comparison with those in the C3A cell line. Interestingly, the obtained results revealed that NH_4Cl elevated albumin mRNA levels both in genetically modified cells and in their unmodified counterparts. The relative value of *Alb* gene expression after ammonium chloride treatment was 1.6-fold higher for C3A_AO_P2A, 3.3-fold ($p < 0.001$) higher for C3A_AO, and 1.5-fold higher for C3A cells (Fig. 2c).

In the case of other genes analyzed at the mRNA level, when comparing C3A_AO_P2A with C3A cells, downregulation of the expression of the *HNF4A*, *HSPA1A*, and *NF-κB* genes was observed. In turn, C3A_AO cells were characterized by 5.9-fold ($p = 0.032$) and 4.2-fold ($p = 0.016$) higher expression of the *HNF4A* gene than C3A_AO_P2A and C3A cell lines, respectively. Moreover, the *HNF1A* gene was also upregulated in C3A_AO compared with C3A_AO_P2A and C3A by 2.5-fold and 3.1-fold, respectively (Fig. 2c).

RT-qPCR analysis demonstrated also upregulation of the *HSPA1A* heat-shock protein gene in all analyzed cell lines after ammonium chloride treatment. This upregulation confirms that the NH_4Cl treatment induced oxidative/nitrosative stress (Fig. 2c).

3.2. Genetically modified HCC cells secrete more albumin

Quantitative measurements of albumin synthesis (ELISA) in static culture indicated that genetically modified cells, C3A_AO, produced the highest amounts of the protein when calculated per number of living cells. In turn, the lowest synthesis was observed for the C3A_AO_P2A cell line. On the third day of culture, C3A_AO produced 1.3-fold and 1.5-fold higher albumin than C3A and C3A_AO_P2A cells, respectively. In turn, on the 6th day, genetically modified and unmodified cell lines were characterized by similar synthesis of the analyzed protein. The reason for this can be explained by significant differences in the number of living cells between three independent biological repetitions. Averaged results for C3A and C3A_AO_P2A cells are characterized by high standard deviation and therefore it is difficult to make any comparison. The results obtained on the following days revealed that C3A_AO outperformed the other two HCC cell lines in albumin secretion. Production of analyzed protein by C3A_AO cells on the 9th day was 1.5-fold ($p = 0.008$) and 1.7-fold ($p = 0.002$) higher than by C3A and C3A_AO_P2A, respectively. Similar results were obtained on the 12th day of culture. As expected, albumin production by the HOS cell line was not observed (Fig. 3a).

3.3. C3A_AO_P2A cells produce more urea

Quantitative measurements of urea production in media samples revealed that the newly established C3A_AO_P2A cell line was characterized by the highest production of the analyzed metabolite. The results obtained for unmodified C3A cells and for the older version of genetically modified HCC cells - C3A_AO were 1.2-fold ($p = 0.047$) and 2.5-fold ($p < 0.001$) lower in comparison with C3A_AO_P2A cells. Interestingly, the urea measurements in cell lysates revealed different results. The highest amounts of urea were found in C3A_AO cells. When compared with C3A_AO cells, the results obtained for C3A and C3A_AO_P2A cells were 1.5-fold ($p < 0.001$) and 2.1-fold ($p < 0.001$) lower. Nevertheless, after summing up the mass of urea measured in the medium and in the cell lysates, C3A_AO_P2A cells showed the highest production of total urea per number of living cells, and C3A_AO showed the lowest. The comparison of the results obtained from the HCC cells to the measurements conducted on liver cell isolate showed that the human HCC cells had significantly lower urea production. Specifically, the HCC cells had approximately 20-fold lower urea production in cell lysates and 100-fold lower urea production in culture medium, as shown in Fig. 3b.

3.4. Genetically modified cells are more resistant to oxidative/nitrosative stress

Cell viability, metabolic activity, and ability to synthetize albumin under ammonia-induced stress were evaluated for 3 versions of human HCC cell lines. Measurements of albumin secretion (ELISA) indicated that the presence of ammonium chloride induced synthesis of the protein by human HCC cells. Both genetically modified cell lines produced higher amounts of albumin than their parental C3A cells when calculated per number of living cells. The highest secretion of this protein was observed for C3A_AO cells. Under standard conditions, albumin production by C3A_AO cells was 1.6-fold ($p < 0.001$) and 1.5-fold ($p = 0.002$) higher than that by C3A and C3A_AO_P2A cells, respectively. After treatment with 20 mM ammonium chloride, the synthesis of the analyzed protein by both genetically modified cell lines was similar, and the differences were not statistically significant. In turn, albumin production by C3A cells was 1.3-fold ($p = 0.009$) and 1.2-fold ($p = 0.035$) lower than that by C3A_AO and C3A_AO_P2A, respectively. Finally, after treatment with 40 mM ammonium chloride, C3A_AO cells were characterized by 1.9-fold ($p < 0.001$) and 1.2-fold ($p = 0.033$) higher albumin secretion than C3A and C3A_AO_P2A cells, respectively. Again, albumin production by HOS cells was not observed (Fig. 3c).

Cytometric analysis (FACS) revealed that the highest effect on the percentage of dead cells after exposure to different concentrations of NH_4Cl was observed for C3A cells. The analyzed parameter increased more than 3-fold after treatment with 20 mM and 40 mM solutions of

a

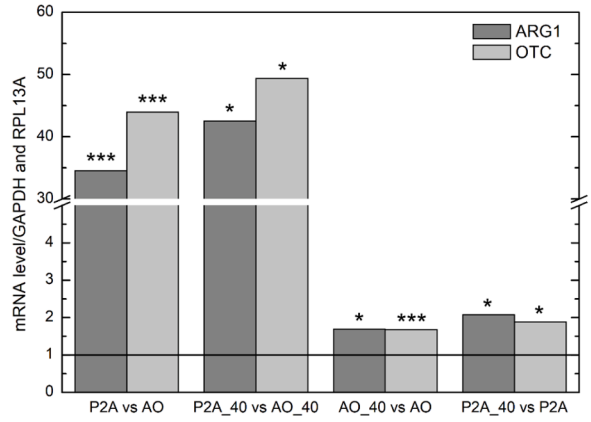

b

	ARG1	*OTC*
P2A vs AO	34.534 (<0.001)	43.970 (<0.001)
P2A_40 vs AO_40	42.536 (0.022)	49.406 (0.025)
P2A_40 vs P2A	2.080 (0.024)	1.883 (0.015)
AO_40 vs AO	1.689 (0.036)	1.676 (0.001)

c

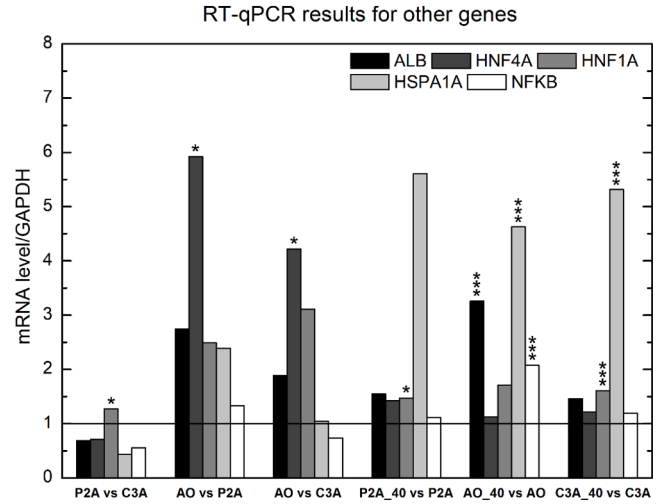

d

	ALB	*HNF4A*	*HNF1A*	*HSPA1A*	*NFKB*
P2A vs C3A	0.689 (0.176)	0.713 (0.084)	1.272 (0.016)	0.437 (0.093)	0.557 (0.067)
AO vs P2A	2.742 (0.398)	5.922 (0.032)	2.491 (0.766)	2.39 (0.936)	1.329 (0.713)
AO vs C3A	1.888 (0.593)	4.221 (0.016)	3.107 (0.068)	1.044 (0.916)	0.74 (0.665)
P2A_40 vs P2A	1.545 (0.150)	1.417 (0.587)	1.469 (0.036)	5.607 (0.053)	1.113 (0.502)
AO_40 vs AO	3.259 (<0.001)	1.125 (0.475)	1.711 (0.099)	4.628 (<0.001)	2.073 (<0.001)
C3A_40 vs C3A	1.455 (0.117)	1.215 (0.224)	1.606 (<0.001)	5.314 (<0.001)	1.192 (0.309)

(caption on next column)

Fig. 2. Comparison of genetically modified cells – C3A_AO and C3A_AO_P2A with their parental C3A cell line – analysis of the expression of selected genes at the mRNA level. Results of RT-qPCR experiments conducted for C3A, C3A_AO_P2A, and C3A_AO cells cultured with or without 40 mM NH_4Cl. To determine the changes in mRNA levels, REST 2009 software and the Pfaffl model were used. **(a)** Analysis of the expression of *ARG1* and *OTC* transgenes in genetically modified hepatic cells. Data normalization was performed using the *RPL13A* and *GAPDH* genes. Number of biological repeats: 4. **(b)** Statistical significance (p) for Fig. 2a. **(c)** Analysis of the expression of *ALB*, *HNF1A*, *HSP1A1*, *HNF4A*, and *NF-κB* genes in human HCC cells. Data normalization was performed using the *GAPDH* gene. Number of biological repeats: 3. **(d)** Statistical significance (p) for Fig. 2c. Abbreviations: AO - C3A_AO; P2A - C3A_AO_P2A. All experiments were performed according to the MIQE guidelines. Levels of significance: $p < 0.05$ (*); $p < 0.01$ (**); $p < 0.001$ (***).

ammonium chloride. In turn, the cell viability of genetically modified cells was much less affected. The percentage of dead cells increased less than 2-fold after exposure to two different concentrations of NH_4Cl, which confirmed that C3A_AO and C3A_AO_P2A cells are significantly more resistant to oxidative/nitrosative stress. HOS cells were not affected by NH_4Cl treatment (Fig. 3d).

In the case of cell metabolic capacity, treatment with different concentrations of NH_4Cl (20 mM, 40 mM, and 60 mM) had an effect on mitochondrial activity, which decreased with increasing concentration. The strongest impact was observed for unmodified C3A cells. In turn, the genetically modified cell lines were more resistant to ammonia-induced stress. The results of this analysis also indicated that mitochondrial activity in a control HOS cell line was much less affected by NH_4Cl treatment (Fig. 3e).

3.5. *Characterization of polysulfone capillary membrane used for the development of the system for dynamic culture (model of BAFBBAL)*

Evaluation of the structure (porosity, pore size etc.) of the chosen polysulfone membrane was conducted using SEM. The results of microscopic analysis revealed that the structure of the membrane is varied. The closer to the intracapillary space of the membrane the pores are larger. The size of the pores of the external structure was evaluated to compare with the value of this parameter declared by the producer (0.2 μm). One hundred measurements were made and presented as the average. The obtained results indicated that the pore size of the polysulfone membrane equaled 0.26 μm (±0.08). Moreover, the external and internal diameters were dimensioned. The results of the conducted measurements were 588 μm (±24) and 400 μm (±38.5), respectively (Fig. 4a).

To define the cutoff point for the polysulfone capillary membrane, retention measurements were conducted. The studies confirmed that molecules smaller than 200 nm pass, either completely in the case of bovine serum albumin, or partially (in the case of polystyrene microspheres with a particle size of 100 nm) through the capillary membrane. The results obtained for the larger objects (polystyrene microspheres and beads with particle size ≥ 200 nm) revealed that they were completely retained (Fig. 4b). This indicates that the polysulfone capillary membrane was able to effectively filter out particles with particle size larger than 200 nm.

3.6. *Optimization of dynamic culture conditions*

Optimization of two parameters connected with dynamic culture, cell density and medium flow rate, was conducted using C3A cells. The results indicated that the fastest glucose consumption occurred under static conditions. Depletion of glucose in static culture was observed on the 6th day of culture (starting seeding density: $5{\cdot}10^6$ cells) and on the 10th day of culture (starting seeding density: $0.5{\cdot}10^6$ cells). In turn, during the culture in dynamic conditions conducted in a 20 times larger volume of medium, only half of the glucose was utilized on day 12. In

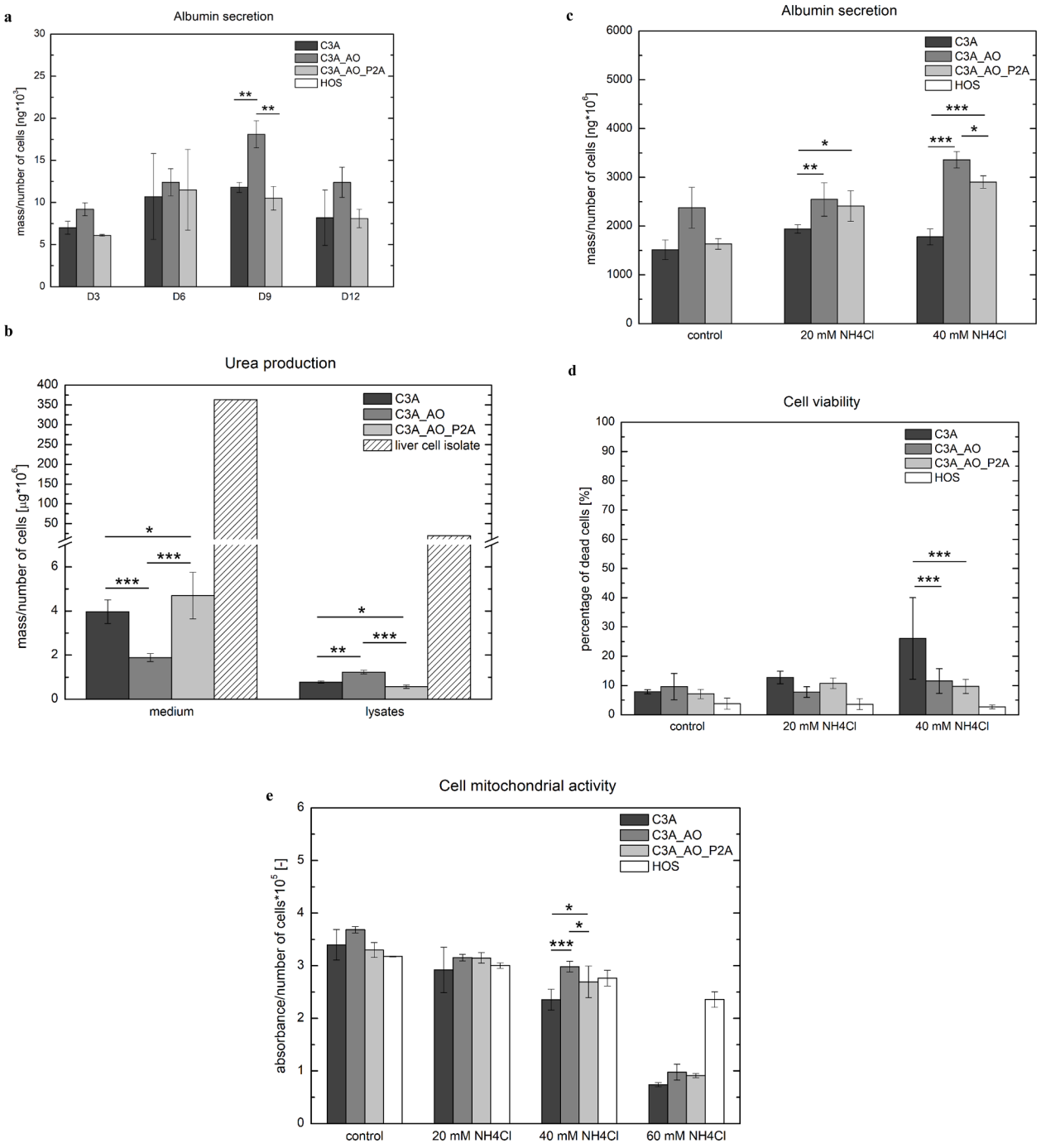

Fig. 3. Comparison of genetically modified cells – C3A_AO and C3A_AO_P2A – with their parental C3A cell line at the functional level. (a) Albumin secretion by human HCC cells was measured in media samples using ELISA. The obtained results were expressed as the ratio of albumin mass per number of living cells. Data represent the mean value ± SD (n = 3). Statistical analysis was conducted using multivariate ANOVA with Duncan's *post hoc* test. Levels of significance: $p < 0.05$ (*); $p < 0.01$ (**); $p < 0.001$ (***). **(b)** Urea production by human HCC cells (after induction with 40 mM NH_4Cl) was evaluated both in cell lysates and in conditioned medium using a QuantiChrom Urea Assay Kit. The results were expressed as the ratio of urea mass per number of living cells. Data represent the mean value ± SD (n = 3). Statistical analysis was conducted using multivariate ANOVA with Duncan's *post hoc* test. Levels of significance: $p < 0.05$ (*); $p < 0.01$ (**); $p < 0.001$ (***). **(c)** Albumin secretion by human HCC cells after 24 h incubation with 20 mM and 40 mM NH_4Cl was measured using ELISA. The results were expressed as the ratio of albumin mass per number of living cells. Data represent the mean value ± SD (n = 3). Statistical analysis was conducted using multivariate ANOVA with Duncan's *post hoc* test. Levels of significance: $p < 0.05$ (*); $p < 0.01$ (**); $p < 0.001$ (***). **(d)** Viability of human HCC cells after treatment with NH_4Cl was determined using propidium iodide (PI) staining and flow cytometry analysis (FACS). Cells were cultured with 20 and 40 mM NH_4Cl for 24 h. The results are expressed as the percentage of dead cells. Data represent the mean value ± SD (n = 4). Statistical analysis was conducted using multivariate ANOVA with Duncan's *post hoc* test. Levels of significance: $p < 0.05$ (*); $p < 0.01$ (**); $p < 0.001$ (***). **(e)** Mitochondrial activity in human HCC cells after treatment with different concentrations of NH_4Cl was determined using the MTT test. C3A cells and their genetically modified counterparts were treated with 20 mM, 40 mM, and 60 mM NH_4Cl for 24 h. Data represent the mean value ± SD (n = 4). Statistical analysis was conducted using multivariate ANOVA with Duncan's *post hoc* test. Levels of significance: $p < 0.05$ (*); $p < 0.01$ (**); $p < 0.001$ (***).

a

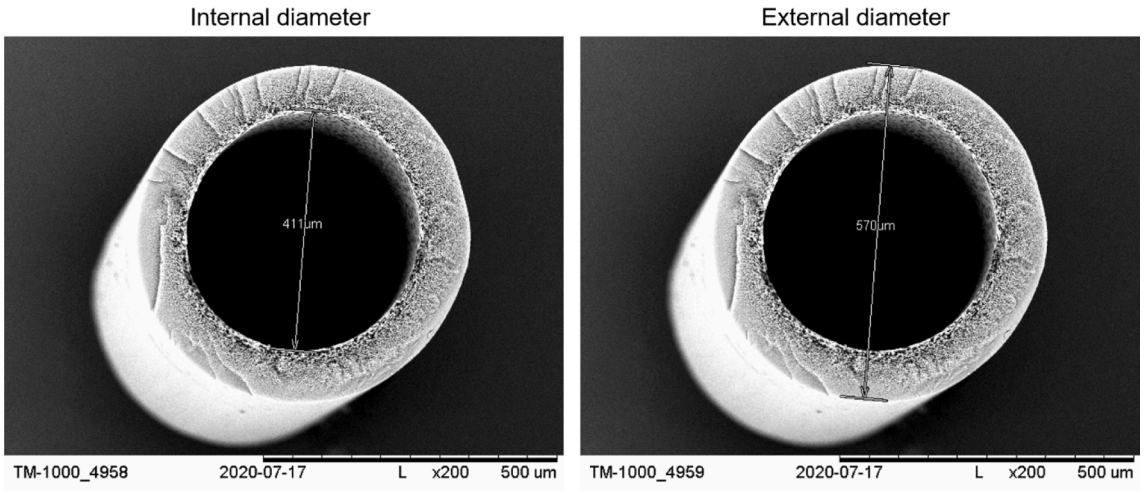

b

Compound	Retention [%]
Bovine albumin (7.1 nm)	2
Red fluorescent polystyrene microspheres (100 nm)	69
Red fluorescent polystyrene microspheres (200 nm)	99
Red fluorescent polystyrene microspheres (500 nm)	100
Cytometer Setup and Tracking Beads (2 µm and 3 µm)	100

Fig. 4. Characterization of polysulfone capillary membranes used for BAFBBAL construction. (a) SEM images representing the cross-section of the polysulfone capillary membrane used in the BAFBBAL model. The images show the dimensions of the internal and external diameters of the membrane. Scale bar: 500 µm. **(b)** The table representing the results of retention measurements for prepared hollow fiber bioreactors.

the case of the culture variant in which ten times fewer cells were seeded, practically no consumption of glucose from the medium was observed. Interestingly, the use of different flow rates (5 mL/min and 10 mL/min) did not significantly affect the rate of glucose usage. In summary, the optimization process revealed that the initial number of seeded cells had a more significant impact on glucose consumption than the medium flow rate (Fig. 5a).

In the case of albumin secretion, both parameters exerted synergistic effects on the production of the analyzed protein. The highest albumin secretion was observed for cells cultured at a 10 mL/min flow rate and with a starting seeding density of $5{\cdot}10^6$ cells per bioreactor. Interestingly, the obtained results indicated a decrease in the amounts of synthesized protein using a 5 mL/min flow rate (with the same initial number of seeded cells) after day 9 of the culture. Analysis of the variant with a starting seeding density of $5{\cdot}10^6$ cells confirmed that dynamic culture ensured greater albumin secretion than static culture. In turn, a 10-fold lower initial number of seeded cells caused the production of the analyzed protein in the flow conditions and in the static cultures to be comparable (Fig. 5b). In summary, for further studies on dynamic hepatic cell cultures, a flow rate of 10 mL/min and a load of $5{\cdot}10^6$ cells were chosen.

3.7. Genetically modified HCC cell lines outperform their parental cell line in dynamic culture conditions

Glucose consumption in dynamic and static conditions was measured in medium samples collected during the culture. The obtained results indicated that human HCC cells completely consumed glucose from the culture medium on the 6th day of static culture. In contrast, during culture in dynamic conditions, only half of the glucose was used. Interestingly, the rate of glucose consumption by the C3A cells and their genetically modified counterparts, expressed as a concentration of the analyte in a medium, was very similar in regards to the same culture conditions (Fig. 6a left panel and 6b left panel). The first biological repetition (Fig. 6a left panel) showed that all cells were metabolically active at similar levels under static conditions, but under dynamic conditions, the C3A cells consumed glucose the most rapidly. In turn, the second biological repetition (Fig. 6b left panel) revealed a similar tendency in the rate of glucose consumption in static conditions, but in dynamic conditions, the C3A_AO_P2A cells consumed glucose faster than their counterparts.

Measurements of the total content of albumin in the medium indicated that under dynamic conditions, human HCC cells produced circa 4 times higher amounts of the protein. Interestingly, in both types of culture, genetically modified cells outperformed their unmodified counterparts in the synthesis of albumin (Fig. 6a right panel and 6b right panel). The first biological repetition (Fig. 6a right panel) showed that C3A_AO_P2A cells produced the highest amounts of albumin in both static and dynamic cultures. A similar tendency in the secretion of this protein was confirmed in the second biological repetition (Fig. 6b right panel). This fact can be explained by, for example, the fastest growth rate exhibited by these cells.

4. Discussion

Liver cell 3D culture carried out in dynamic conditions has many advantages compared to using a 2D static culture. In cultures with media flow, control of parameters such as temperature, pH, and nutrient

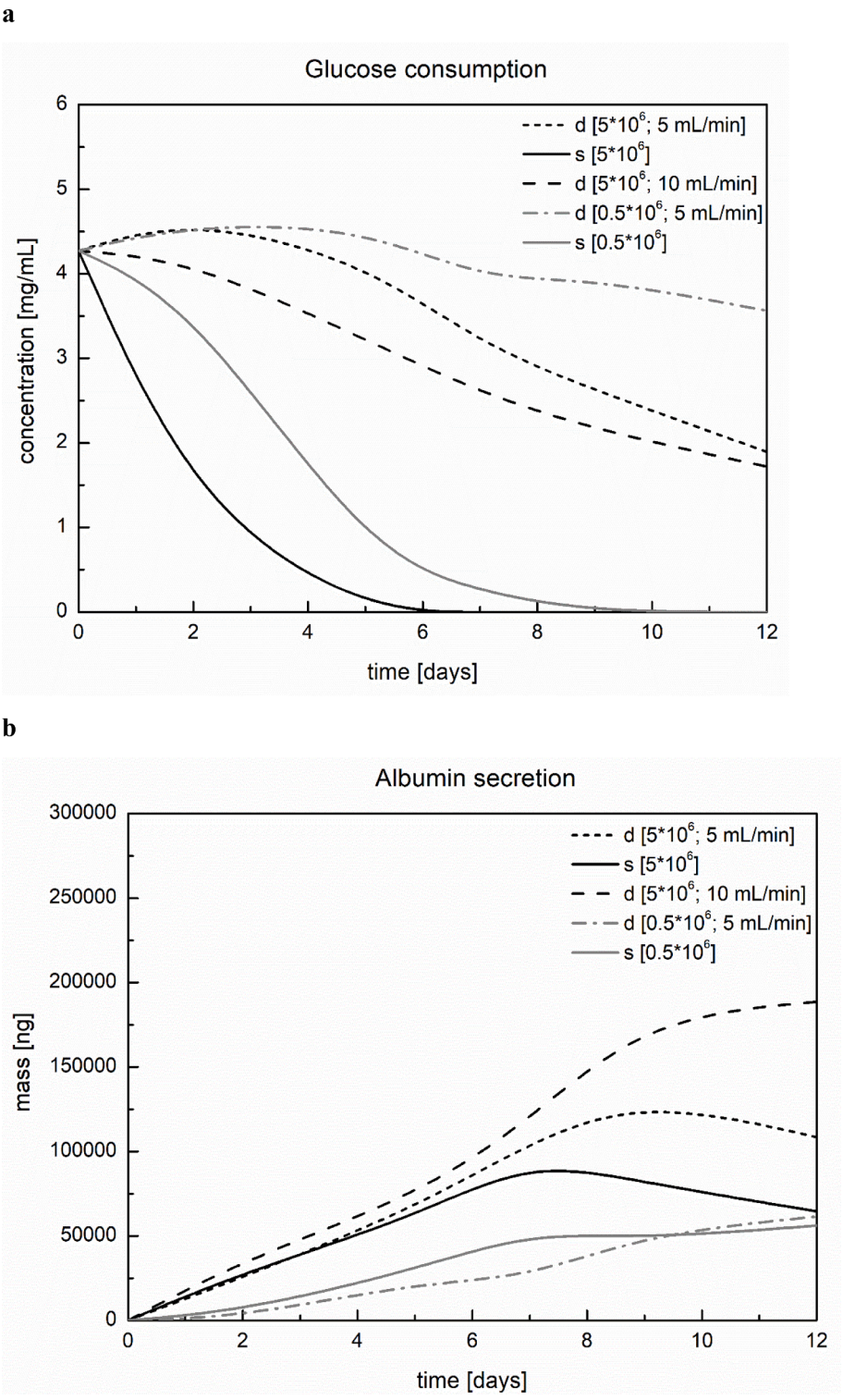

Fig. 5. Optimization of parameters associated with dynamic cell culture. (a) Glucose media content in static and dynamic conditions was evaluated using a commercial kit**.** The effect of using different flow rates and seeding densities on glucose consumption by HCC cells was determined. **(b)** Albumin synthesis by human HCC cells in static and dynamic conditions was measured using ELISA**.** The effect of using different flow rates and seeding densities on the secretion of the analyzed protein was determined. Abbreviations: d – dynamic culture; s – static culture.

exchange is more precise. Under 3D and flow conditions, cell–cell and cell-matrix interactions are ensured, which is limited in a regular monolayer culture. The biological functions of cells are close to those found in native conditions. The polarity of cell membranes (particularly important for hepatocytes), tissue-specific gene expression, and protein production are preserved. Continuous medium perfusion in cell cultures enables the establishment of physiological drug profiles and may be important in drug testing applications. The use of culture medium flow, gas exchange, and the formation of three-dimensional structures by hepatic cells can be used to create *in vitro* tissue models for various applications, e.g., hepatotoxicity/genotoxicity tests and drug discovery [24]. In the context of HCC cell lines, which have some metabolic

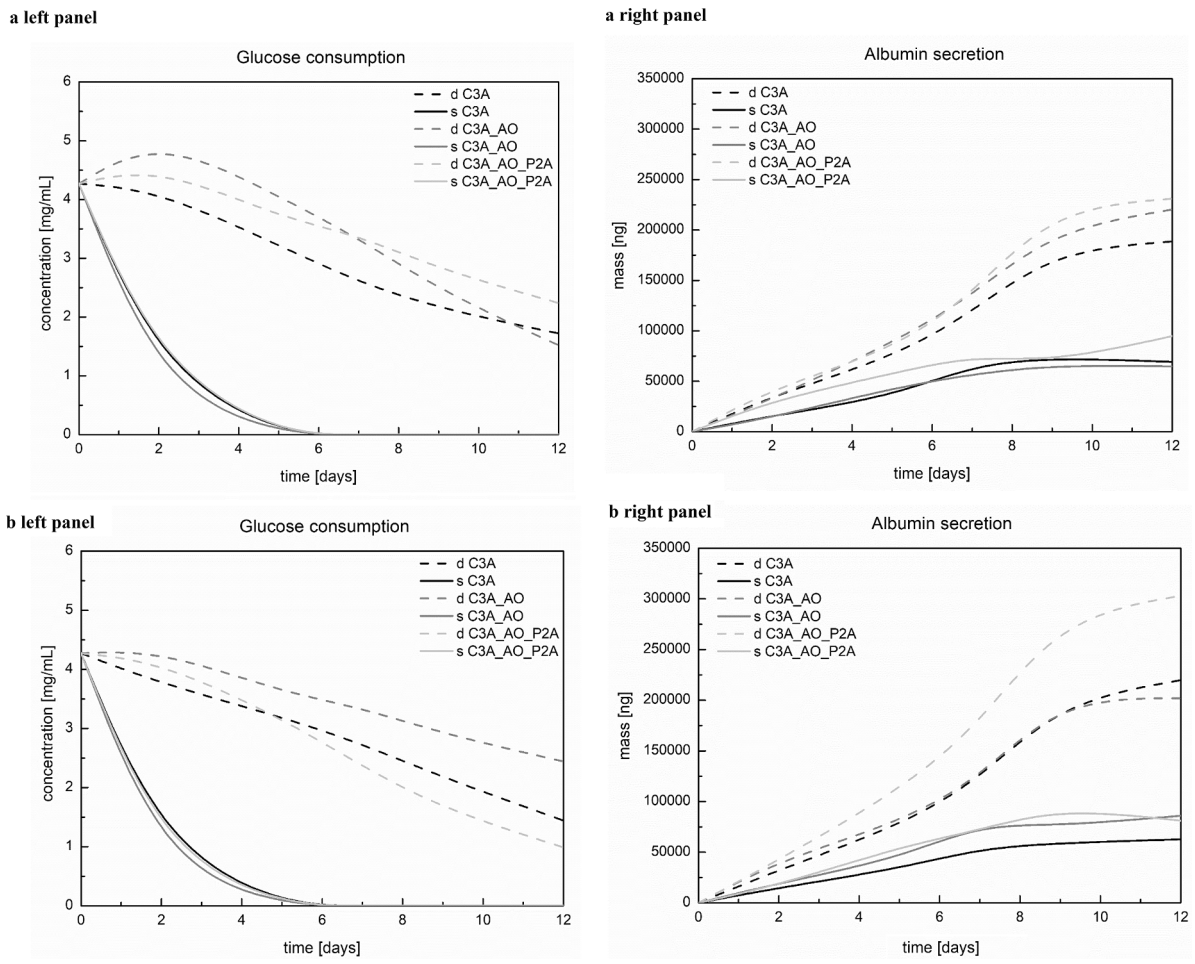

Fig. 6. Comparison of functionality of genetically modified cell lines - C3A_AO and C3A_AO_P2A with their parental C3A cells in dynamic conditions. The final dynamic cultures were conducted using 10 mL/min as the flow rate and $5{\cdot}10^6$/bioreactor as the initial number of seeded cells. Static cultures were set as a control with the same cell density per T25 culture flask. Both types of cultures were conducted simultaneously and lasted for 12 days. **(a)** Comparison of glucose consumption (**left panel**) and albumin secretion (**right panel**) by human HCC cell lines in static and dynamic conditions – first biological repetition. **(b)** Comparison of glucose consumption (**left panel**) and albumin secretion (**right panel**) by human HCC cells in static and dynamic conditions – second biological repetition. Abbreviations: d – dynamic culture; s – static culture.

shortages, including a nonfunctional urea cycle, culturing in dynamic conditions brings significant benefits. The C3A and HepaRG cell lines differentiated markedly in the AMC-BAL flow system compared to monolayer controls, manifested in significant differences in hepatic gene expression levels and carbohydrate-, xenobiotic-, nitrogen-, and amino acid metabolism. The urea cycle enzymes *CPS1* (carbamoyl phosphate synthetase I), *OTC*, and *ARG1* were upregulated (up to 5-fold) when cultured in AMC-BAL. However, urea production in dynamic cultures was circa 3-fold higher for HepaRG when compared to static conditions, yet not different in C3A cultures [18,25].

In the case of the HCC cell lines used in current experiments, we first compared the performance of C3A and its genetically modified derivatives, C3A_AO [21] and its newer version, presented here for the first time, C3A_AO_P2A, in standard monolayer cultures. Both modified cell lines have additional copies (transgenes) of human *OTC* and *ARG1* stably introduced into the cell genome using lentiviral vectors (Supplementary Fig. 1) but were prepared in quite a different way: the former was transduced with two different lentiviral vectors bearing h*OTC* or h*ARG1* and not selected for successful transduction, whereas the latter was modified with a single vector carrying one transcriptional cassette expressing the two transgenes simultaneously (Supplementary materials). As a result, C3A_AO is a mixed population of cells: nontransduced, producing single transcripts, or expressing both transgenes (minority of cells). In turn, C3A_AO_P2A, after antibiotic selection, consisted of nearly 100 % *ARG1*- and *OTC*-expressing cells, hallmarked by significantly higher mRNA levels of transgenes than in its C3A_AO sister cell line (Fig. 2a). C3A_AO was characterized by higher albumin secretion and higher urea content in cell lysates than its parental C3A cell line. Last but not least, C3A_AO cells were more resistant to the oxidative/nitrosative stress induced by the presence of high concentrations of ammonia cations [21]. In this paper, we also show that the older version of genetically modified cells synthesized the greatest amounts of albumin (Fig. 3a), but regarding urea secretion into the medium, the new generation of genetically modified cells, the C3A_AO_P2A cell line, was the most efficient (Fig. 3b). This discrepancy between urea content in cell lysates and in medium among our HCC cell lines probably lies in differences in active urea transport through cell membranes, but its exact mechanism is not yet fully understood [26]. Nevertheless, the new modified cell line produced the greatest total amounts of urea of all three (Fig. 3b), and both cell lines that have additional copies of h*OTC* and h*ARG1* genes are less prone to stress induced by ammonia ions (Fig. 3c, 3d, and 3e). The last mentioned feature of hepatic cells has great importance when clinical applications are considered, where non-physiological concentrations of ammonia are found in patients' blood. Significantly lower urea synthesis by genetically modified cell lines when compared with isolated human liver cells (Fig. 3b) was not expected, especially in the case of C3A_AO_P2A cells characterized by very high mRNA levels of h*ARG1* and h*OTC* transgenes (Fig. 2a). However,

this phenomenon is not reflected in the highly elevated protein synthesis and very high activities of the corresponding urea cycle enzymes (Supplementary Fig. 3a and 3b, and Supplementary Fig. 4, respectively). This situation remains to be clarified. The other problem constitutes the lack or low expression of the *CPS1* gene in the majority of HCC cell lines, including HepG2/C3A [19]. Although we found it slightly upregulated in our modified cell lines (Supplementary Fig. 2), it can still be a bottleneck of urea cycle performance in tested cells.

Additionally, for other liver-specific genes, we observed differences in expression at the mRNA level between modified and unmodified cell lines (Fig. 2c). The expression of the albumin-coding gene under normal conditions was the highest in the C3A_AO cells. This could be explained by the elevated mRNA synthesis of the *HNF4A* and *HNF1A* genes in these cells. Both genes encode liver-related transcription factors involved in the regulation of serum albumin levels [27]. On the other hand, only *HNF1A* is upregulated in the C3A_AO_P2A cell line compared to C3A. Nagaki and Moriwaki [28] reported that *HNF4A* is a positive regulator and activator of *HNF1A* expression, which in turn is a global regulator of the transcriptional network involved in maintaining the hepatocyte-specific phenotype. Transfection with the plasmid bearing the *HNF4A* gene resulted in HCC cells with an increase in the expression of *HNF1A* and liver-specific genes such as apolipoproteins, α1-antitrypsin, albumin, and cytochrome P450 families. Interestingly, the upregulation of the *ALB* gene in the presence of NH_4Cl was the most prominent in the C3A_AO cells at both the RNA and protein levels (Fig. 2c, 3c, and Supplementary Fig. 3c). We have shown this phenomenon in our previous report [21], and the degree of this induction also outperformed those exhibited by the new C3A_AO_P2A cell line. In turn, the ammonia-induced expression of *NF-κB* can be responsible for the elevated expression of urea cycle transgenes in C3A_AO cells, since the CMV promoter, used by us to express these genes, is activated in stress conditions *via* this transcription factor [29]. However, despite NH_4Cl-induced *ARG1* and *OTC* activation (Fig. 2a), *NF-κB* was not significantly elevated in C3A_AO_P2A cells (Fig. 2c). Thus, the correlations between gene expression and cell line performance need to be further explored.

In the next step, we focused on the performance of the genetically modified cell lines in dynamic culture conditions, as they are applied in hybrid liver-support systems called BAL. First, we constructed a model of BAFBBAL (Fig. 1) using self-made culture modules with polysulfone capillaries (Fig. 4a). These capillaries have been thoroughly tested for their physical parameters and biocompatibility. The crucial parameter of the membranes used in cell culture is the size of the pores, which defines proper mass transfer [30]. Our capillaries enabled virtually free bidirectional transmembrane traffic of all nutrients and proteins with a size below 100 nm (Fig. 4a and 4b). The polysulfone used for their production had no negative influence on the tested cell performance (Supplementary Fig. 5), and the physical parameters of aqueous solution flow through the capillaries were also convenient for cell culturing (Supplementary Fig. 6 and 7). Second, optimal dynamic culture conditions were established using C3A cells. As judged by glucose consumption and albumin secretion, the medium flow rate was set to 10 mL/min, and the initial cell seeding density was $5{\cdot}10^6$ cells/module (Fig. 5a and 5b). In each of the two independent experiments (biological repetitions), three individual BAFBBALs were run for 12 days to compare the performance of C3A, C3A_AO, and C3A_AO_P2A cell lines in dynamic culture conditions. For the control, cells were simultaneously cultured in static conditions. The seeding density for these controls was also $5{\cdot}10^6$ cells/flask, as the growth surface area was similar for the T25 flask and for 20 capillaries contained in each bioreactor (circa 22 cm^2). As the main culture performance parameters, glucose usage and albumin production were measured in a medium every 2–3 days. We were unable to determine the urea content in the dynamic culture since it was too dilute to be detected in 120 mL of medium. In the initial experiments carried out to compare ability of the cell lines to synthetize urea in static conditions (Section 3.3 of the Manuscript) we cultured cells for 24 h in the medium containing urea cycle substrate (40 mM NH_4Cl), subsequently replaced with the culture medium with reduced content of FBS (Section 2.4). Thus, our method to measure urea content in a medium must be optimized to be compatible with dynamic cell cultures.

The levels of expression of the *ALB* gene or the analysis of the cell capacity to produce albumin is one of the most commonly used indicators of hepatic function [31]. Many reports have confirmed that the 3D culture of hepatic cells results in an increase in the expression of the *ALB* gene [32,33]. Observations of cells grown in our bioreactors suggest that some of the cells formed a monolayer on the hollow fiber surface, but the others formed surface-free cell aggregates resembling spontaneous spheroids. In control static cultures, cell monolayer quickly achieved confluence, which lead to contact inhibition. This inhibition stopped cell growth and slowed down cell physiology. This might occur independently of medium volume. Nevertheless, large amount of medium used for dynamic culture eliminates the need for medium exchange during an extended culture time. We believe that the increase in albumin production in bioreactors, up to 6-fold, compared to static controls (Fig. 6a right panel and 6b right panel), is partly due to the establishment of the 3D cell culture environment, which provides homotypic cell–cell interactions that are very important for hepatocytes [34]. The other factors that might enhance the liver-specific functions of the tested HCC cells in our model are nonlimited glucose in a much larger volume of medium and, connected with this fact, better growth conditions in an environment that ensures better availability of nutrients and faster gas exchange. Last but not least, the medium flow within capillaries additionally provides moderate shear stress, typical of the native hepatocyte environment. Nevertheless, in both types of culture, genetically modified cells outperformed their unmodified counterparts in the synthesis of albumin, calculated as the total medium albumin content (mass). The first biological repetition (Fig. 6a right panel) showed that C3A_AO_P2A cells produced the highest amounts of albumin in both static and dynamic cultures. A similar tendency in the secretion of this protein was confirmed in the second biological repetition (Fig. 6b right panel). As the capacity to produce albumin by the whole bioreactor is more important than individual cell efficiency in such applications as BAL and the new genetically modified cell line is resistant to ammonia-induced stress to a similar degree as C3A_AO cells but produces significantly greater amounts of urea, we postulate such a dynamic culture of C3A_AO_P2A as a novel method of BAL construction.

5. Conclusions

The novelty of our approach to the design of the biologically active function block of the improved BAL lies in the use of the dynamic culture of genetically modified HCC cells. It is important to note that gene transfer using lentiviral vectors is very well studied and considered safe for clinical applications [35]. In 2017, the U.S. Food and Drug Administration (FDA) approved CD19-targeted CAR T-cell therapy (Kymriah™, Novartis) for the treatment of refractory pre-B-cell acute lymphoblastic leukemia [Web ref. 1]. This CAR T-cell-based treatment is the first form of gene transfer therapy to gain commercial approval by the FDA [Web ref. 2], and the autologous T cells were engineered using lentiviral vectors. In our experiments, the use of the genetically modified cells in dynamic culture resulted in increased levels of albumin production compared to the monolayer culture conducted under static conditions. Importantly, the most promising results were obtained in the C3A_AO_P2A culture carried out in hollow fiber bioreactors. Due to the fact that the capillary bioreactors enable mimicking *in vivo* flow conditions and have significant application potential, research toward establishing a successful dynamic coculture of new C3A_AO_P2A cells with feeder layer cells, e.g., genetically modified fibroblasts [36] will be our next step. The urea cycle performance in the C3A_AO_P2A cells requires further improvement. We are planning to introduce the *CPS1* transgene into their genome and test the effect of this third gene addition on urea cycle functionality. HCC cells with improved liver-specific functions cultured in medium flow can also be extremely useful in

other recently developing applications, such as 3D bioprinted models for antitumor drug discovery [37] or integrated biosensors in microfluidic devices for cytotoxicity testing [31], also called lab-on-chip (LOC).

Declaration of competing interest

The authors declare that they have no known competing financial interests or personal relationships that could have appeared to influence the work reported in this paper.

Appendix A. Supplementary material

Supplementary data to this article can be found online at https://doi.org/10.1016/j.bbe.2023.11.003.

References

[1] Marcellin P, Kutala BK. Liver diseases: A major, neglected global public health problem requiring urgent actions and large-scale screening. Liver Int 2018;38 (Suppl 1):2–6. https://doi.org/10.1111/liv.13682.

[2] Bernal W, Auzinger G, Dhawan A, Wendon J. Acute liver failure. Lancet 2010;376 (9736):190–201. https://doi.org/10.1016/S0140-6736(10)60274-7.

[3] Kadyk LC, Collins LR, Littman NJ, Millan MT. Proceedings: Moving toward cell-based therapies for liver disease. Stem Cells Transl Med 2015;4(3):207–10. https://doi.org/10.5966/sctm.2014-0276.

[4] Meirelles Júnior RF erreir., Salvalaggio P, Rezende MBd, Evangelista AS, Guardia BD ell., Matielo CEL, et al. Liver transplantation: history, outcomes and perspectives. Einstein (Sao Paulo) 2015;13(1):149–52. https://doi.org/10.1590/S1679-45082015RW3164.

[5] García Martínez JJ, Bendjelid K. Artificial liver support systems: what is new over the last decade? Ann Intensive Care 2018;8:109. https://doi.org/10.1186/s13613-018-0453-z.

[6] Stange J. Extracorporeal liver support. Organogenesis 2011;7(1):64–73. https://doi.org/10.4161/org.7.1.14069.

[7] Kribben A, Gerken G, Haag S, Herget-Rosenthal S, Treichel U, Betz C, et al. Effects of fractionated plasma separation and adsorption on survival in patients with acute-on-chronic liver failure. Gastroenterology 2012;142(4):782–789.e3. https://doi.org/10.1053/j.gastro.2011.12.056.

[8] Bañares R, Nevens F, Larsen FS, Jalan R, Albillos A, Dollinger M, et al. Extracorporeal albumin dialysis with the molecular adsorbent recirculating system in acute-on-chronic liver failure: the RELIEF trial. Hepatology 2013;57(3): 1153–62. https://doi.org/10.1002/hep.26185.

[9] Pluta KD, Ciezkowska M, Wisniewska M, Wencel A, Pijanowska DG. Cell-based clinical and experimental methods for assisting the function of impaired livers – Present and future of liver support systems. Biocybern Biomed Eng 2021;41(4): 1322–46. https://doi.org/10.1016/j.bbe.2021.06.005.

[10] Zakrzewska KE, Samluk A, Wencel A, Dudek K, Pijanowska DG, Pluta KD. Liver tissue fragments obtained from males are the most promising source of human hepatocytes for cell-based therapies – flow cytometric analysis of albumin expression. PLoS One 2017;12(8):e0182846.

[11] Lee JH, Park HJ, Kim YA, Lee DH, Noh JK, Jung JG, et al. Establishment of a serum-free hepatocyte cryopreservation process for the development of an "Off-the-Shelf" bioartificial liver system. Bioengineering 2022;9(12):738. https://doi.org/10.3390/bioengineering9120738.

[12] Rowe C, Gerrard DT, Jenkins R, Berry A, Durkin K, Sundstrom L, et al. Proteome-wide analyses of human hepatocytes during differentiation and dedifferentiation. Hepatology 2013;58(2):799–809. https://doi.org/10.1002/hep.26414.

[13] Demetriou AA, Brown RS, Busuttil RW, Fair J, McGuire BM, Rosenthal P, et al. Prospective, randomized, multicenter, controlled trial of a bioartificial liver in treating acute liver failure. Ann Surg 2004;239(5):660–70. https://doi.org/10.1097/01. sla.0000124298.74199.e5.

[14] Teperman L. The ELAD Study Group. Bilirubin Improvement correlates with 90-day survival with use of the ELAD systemin a randomized, controlled study of subjects with acute alcoholic hepatitis or acute decompensation of cirrhosis [abstract]. Am J Transplant 2013;13(Suppl 5):147.

[15] Filippi C, Keatch SA, Rangar D, Nelson LJ, Hayes PC, Plevris JN. Improvement of C3A cell metabolism for usage in bioartificial liver support systems. J Hepatol 2004;41(4):599–605. https://doi.org/10.1016/j.jhep.2004.06.012.

[16] Mavri-Damelin D, Eaton S, Damelin LH, Rees M, Hodgson HJF, Selden C. Ornithine transcarbamylase and arginase I deficiency are responsible for diminished urea cycle function in the human hepatoblastoma cell line HepG2. Int J Biochem Cell Biol 2007;39(3):555–64. https://doi.org/10.1016/j.biocel.2006.10.007.

[17] Mavri-Damelin D, Damelin LH, Eaton S, Rees M, Selden C, Hodgson HJF. Cells for bioartificial liver devices: The human hepatoma-derived cell line C3A produces urea but does not detoxify ammonia. Biotechnol Bioeng 2008;99(3):644–51. https://doi.org/10.1002/bit.21599.

[18] van Wenum M, Adam AAA, Hakvoort TBM, Hendriks EJ, Shevchenko V, van Gulik TM, et al. Selecting cells for bioartificial liver devices and the importance of a 3D culture environment: A functional comparison between the HepaRG and C3A cell lines. Int J Biol Sci 2016;12(8):964–78. https://doi.org/10.7150/ijbs.15165.

[19] Missiaen R, Anderson NM, Kim LC, Nance B, Burrows M, Skuli N, et al. GCN2 inhibition sensitizes arginine-deprived hepatocellular carcinoma cells to senolytic treatment. Cell Metab 2022;34(8):1151–1167.e7. https://doi.org/10.1016/j.cmet.2022.06.010.

[20] Thompson J, Jones N, Al-Khafaji A, Malik S, Reich D, Munoz S, et al. Extracorporeal cellular therapy (ELAD) in severe alcoholic hepatitis: A multinational, prospective, controlled, randomized trial. Liver Transplant 2018;24 (3):380–93. https://doi.org/10.1002/lt.24986.

[21] Pluta KD, Samluk A, Wencel A, Zakrzewska KE, Gora M, Burzynska B, et al. Genetically modified C3A cells with restored urea cycle for improved bioartificial liver. Biocybern Biomed Eng 2020;40(1):378–87. https://doi.org/10.1016/j.bbe.2019.12.006.

[22] Bustin SA, Benes V, Garson JA, Hellemans J, Huggett J, Kubista M, et al. The MIQE guidelines: minimum information for publication of quantitative real-time PCR experiments. Clin Chem 2009;55(4):611–22. https://doi.org/10.1373/clinchem.2008.112797.

[23] Pfaffl MW, Horgan GW, Dempfle L. Relative expression software tool (REST©) for group-wise comparison and statistical analysis of relative expression results in real-time PCR. Nucleic Acids Res 2002;30(9):e36.

[24] Anton D, Burckel H, Josset E, Noel G. Three-dimensional cell culture: A breakthrough in vivo. Int J Mol Sci 2015;16(3):5517–27. https://doi.org/10.3390/ijms16035517.

[25] Moedas MF, Adam AAA, Farelo MA, IJlst L, Chamuleau RAFM, Hoekstra R, et al. Advances in methods for characterization of hepatic urea cycle enzymatic activity in HepaRG cells using UPLC-MS/MS. Anal Biochem 2017;535:47–55. https://doi.org/10.1016/j.ab.2017.07.025.

[26] Jelen S, Gena P, Lebeck J, Rojek A, Praetorius J, Frokiaer J, et al. Aquaporin-9 and urea transporter-A gene deletions affect urea transmembrane passage in murine hepatocytes. Am J Physiol - Gastrointest Liver Physiol 2012;303(11):1279–87. https://doi.org/10.1152/ajpgi.00153.2012.

[27] Guzman-Lepe J, Cervantes-Alvarez E, Collin de l'Hortet A, Wang Y, Mars WM, Oda Y, et al. Liver-enriched transcription factor expression relates to chronic hepatic failure in humans. Hepatol Commun 2018;2(5):582–94. https://doi.org/10.1002/hep4.1172.

[28] Nagaki M, Moriwaki H. Transcription factor HNF and hepatocyte differentiation. Hepatol Res 2008;38(10):961–9. https://doi.org/10.1111/j.1872-034X.2008.00367.x.

[29] Speir E. Cytomegalovirus gene regulation by reactive oxygen species. Agents in atherosclerosis. Ann N Y Acad Sci 2000;899(1):363–74.

[30] Gautier A, Ould-Dris A, Dufresne M, Paullier P, Von Harten B, Lemke HD, et al. Hollow fiber bioartificial liver: Physical and biological characterization with C3A cells. J Memb Sci 2009;341(1–2):203–13. https://doi.org/10.1016/j.memsci.2009.06.007.

[31] de Hoyos-Vega JM, Hong HJ, Stybayeva G, Revzin A. Hepatocyte cultures: From collagen gel sandwiches to microfluidic devices with integrated biosensors. APL Bioeng 2021;5(4):041504. https://doi.org/10.1063/5.0058798.

[32] Coltman NJ, Coke BA, Chatzi K, Shepherd EL, Lalor PF, Schulz-Utermoehl T, et al. Application of HepG2/C3A liver spheroids as a model system for genotoxicity studies. Toxicol Lett 2021;345:34–45. https://doi.org/10.1016/j.toxlet.2021.04.004.

[33] Štampar M, Breznik B, Filipič M, Žegura B. Characterization of in vitro 3D cell model developed from human hepatocellular carcinoma (HepG2) cell line. Cells 2020;9(12):2557. https://doi.org/10.3390/cells9122557.

[34] Li CY, Stevens KR, Schwartz RE, Alejandro BS, Huang JH, Bhatia SN. Micropatterned cell-cell interactions enable functional encapsulation of primary hepatocytes in hydrogel microtissues. Tissue Eng - Part A 2014;20(15–16): 2200–12. https://doi.org/10.1089/ten.tea.2013.0667.

[35] Pluta K, Kacprzak MM. Use of HIV as a gene transfer vector. Acta Biochim Pol 2009;56(4):531–95.

[36] Wencel A, Ciezkowska M, Wisniewska M, Zakrzewska KE, Pijanowska DG, Pluta KD. Effects of genetically modified human skin fibroblasts, stably overexpressing hepatocyte growth factor, on hepatic functions of cocultured C3A cells. Biotechnol Bioeng 2021;118(1):72–81. https://doi.org/10.1002/bit.27551.

[37] Sun L, Yang H, Wang Y, Zhang X, Jin B, Xie F, et al. Application of a 3D bioprinted hepatocellular carcinoma cell model in antitumor drug research. Front Oncol 2020; 10:878. https://doi.org/10.3389/fonc.2020.00878.